Evaluation of a sponge assisted-granular anaerobic membrane bioreactor (SG-AnMBR) for municipal wastewater treatment

C. Chen[a], W.S. Guo[a*], H. H. Ngo[a], Y. Liu[a], B. Du[b], Q. Wei[c], D. Wei[b], D. D. Nguyen[d], S. W. Chang[d]

[a] Centre for Technology in Water and Wastewater, School of Civil and Environmental Engineering, University of Technology Sydney, NSW 2007, Australia

[b] School of Resources and Environment, University of Jinan, Jinan 250022, PR China

[c] Key Laboratory of Chemical Sensing & Analysis in Universities of Shandong, School of Chemistry and Chemical Engineering, University of Jinan, Jinan 250022, PR China

[d]Department of Environmental Energy & Engineering, Kyonggi University, 442-760, Republic of Korea

* Corresponding author: Email: wguo@uts.edu.au, Tel: +61 (2) 95142739, Fax: + 61(2) 95147803

Abstract

This study compared a conventional granular anaerobic membrane bioreactor (CG-AnMBR) with a sponge assisted-granular anaerobic membrane bioreactor (SG-AnMBR) in terms of treatment performance, granular sludge properties, membrane fouling behaviour and biogas production. The SG-AnMBR showed better organics and nutrient removal, and enhanced methane yield at 156.3 ± 5.8 mL $CH_{4\ (STP)}$/g $COD_{removed}$. Granular sludge from the SG-AnMBR had superior quality with better settleability, larger particle size, higher EPS content and more granule abundance. The SG-AnMBR also exhibited slower fouling development with 50.7% lower total filtration resistance than those of the CG-AnMBR. Sponge addition effectively affected the concentration and properties of microbial products (e.g. soluble microbial products (SMP) and extracellular polymeric substances (EPS)) in granular sludge, cake layer as well as settling zone mixed liquor, thus alleviating the fouling propensity. The liquid chromatography-organic carbon detection (LC-OCD) analysis suggested that sponge

addition reduced the concentrations of biopolymers, low molecular weight neutrals and acids, and building blocks of the foulants. Compared with the SG-AnMBR, GC-MS analysis confirmed the accumulation of volatile fatty acids, particularly acetic acid in the CG-AnMBR. It is evident that the SG-AnMBR could be a promising solution for improving overall G-AnMBR performance and substantially mitigating membrane fouling.

Keywords: Anaerobic membrane bioreactor (AnMBR); Sponge; Granular sludge; Membrane fouling; Biogas production

1. Introduction

In the past decades, anaerobic membrane bioreactors (AnMBRs) have been found particularly attractive for wastewater treatment because it can not only achieve total biomass retention, high effluent quality, small footprint and low sludge production, but also significantly contribute to renewable bioenergy generation for the substitution of fossil fuel in power and heat production [1-4]. In particular, granular anaerobic membrane bioreactor (G-AnMBR), a hybrid anaerobic bioreactor incorporating granular technology with membrane based separation, offers a promising approach compared to the conventional anaerobic membrane bioreactor (C-AnMBR) predominantly in the form of continuous stirred tank reactor configuration. The competitive advantages of G-AnMBR include no requirement for mechanical mixing, significantly low energy demand and much more compact reactor design [5].

Contrary to conventional suspended growth bioflocs, anaerobic granules have regular and well-defined shape, strong structure, and good settling velocities, which can enable high biomass retention and withstand high strength wastewater and shock loadings, and produce biogas [6, 7]. The granule bed systems are usually featured with total biomass concentrations ranging from 20 to 40 g/L. All the biological reactions occurred within the dense granular sludge bed at the bottom of the anaerobic granular bioreactor. In a G-AnMBR, membrane module is not directly exposed to the bulk sludge and rather immersed in the sludge supernatant. Thus, the potential effects of suspended solids on membrane fouling can be reduced to some extent due to less apparent cake layer build-up and its consolidation compared to the C-AnMBR [8]. Garcia et al. [9] compared filtration performance of a G-AnMBR with a C-AnMBR when treating domestic wastewater. They observed that the G-AnMBR exhibited notably lower fouling rate, as the G-AnMBR demonstrated low concentrations of mixed liquor suspended solids (MLSS), and 50% less of SMP (soluble microbial products) concentration. In addition, Garcia et al. [10] reported lower fouling potential could be achieved in the G-AnMBR, which was attributed to the reduced solid and colloidal loading (by a factor of 10 and 3) on the membrane. Less fouling in G-AnMBR also ensured enhanced operation with increased fluxes and reduced gas sparging intensity.

However, recent research has shown that the integration of membrane into the granular systems could affect the hydraulics of granular sludge bed by eliminating the washout of fine floc sludge, thereby negatively impacting granular sludge properties [8, 11]. The accumulation of fine and colloidal flocs in sludge supernatant may also contribute to membrane fouling. In addition, at high liquid and biogas upflow velocity,

77 vigorous up and down movements of granules may break granules, resulting in granules
78 fragmentation due to the high shear force [12-14]. It is essential to seek for strategies to
79 maintain the quality of granules for long-term operation of submerged G-AnMBR, since
80 the integrity of the anaerobic granules determines the efficiency and stability of
81 anaerobic biological treatment and guarantees the sludge supernatant quality for
82 controlling fouling propensity.
83
84 The low cost polyutrethane sponge has been considered as an ideal attached growth
85 mobile media in many aerobic submerged MBR studies to improve overall system
86 performance due to its high specific surface area and internal porosity, light weight and
87 high stability to hydrolyse [15]. Guo et al. [16] indicated sponge addition could
88 significantly enhance the treatability of a conventional submerged membrane bioreactor,
89 resulting in 2-time increase in sustainable flux. Additionally, sponge addition into
90 submerged MBR can effectively retain biomass and enhance the flocculation ability of
91 sludge flocs, leading to better membrane fouling mitigation and better nutrient removal
92 [17, 18]. Deng et al. [17] also reported that sponge media could positively modify the
93 sludge flocs, reduce SMP and EPS (extracellular polymeric substances), and prevent
94 cake layer formation and pore clogging, thereby alleviating membrane fouling.
95
96 As far as we know, the effects of sponge, as the inert material, on the enhancement
97 of granular sludge characteristics, and membrane fouling mitigation in the G-AnMBR
98 have yet to be investigated for domestic wastewater treatment. Thus, this study aimed to
99 evaluate the overall performance of a sponge assisted-granular anaerobic membrane
100 bioreactor (SG-AnMBR) and a conventional G-AnMBR (CG-AnMBR). Granule

properties (e.g. particle size distribution (PSD), SMP and EPS, sludge volume index (SVI), etc.), fouling propensity (e.g. transmembrane pressure (TMP), SMP and EPS of the mixed liquor and cake layer, and foulants) and biogas production were also assessed.

2. Materials and methods

2.1. Wastewater

The lab scale experiments were conducted using synthetic wastewater to simulate domestic wastewater just after primary treatment. The synthetic wastewater is comprised of organics and macronutrients such as glucose, ammonium sulphate, potassium dihydrogen phosphate, and trace nutrients. The synthetic wastewater composition was slightly modified based on the previous study of Deng et al. [17] to maintain COD: N: P = 100: 2: 1. The synthetic wastewater contains dissolved organic carbon (DOC) of 100 - 120 mg/L, chemical oxygen demand (COD) of 330 - 370 mg/L, ammonia nitrogen (NH_4^+-N) of 5.5 - 6.6 mg/L, nitrite nitrogen (NO_2^--N) of 0 - 0.02 mg/L, nitrate nitrogen (NO_3^--N) of 0.2 - 0.8 mg/L, and orthophosphate (PO_4^{3-}-P) of 3.1 - 3.6 mg/L. $NaHCO_3$ or NaOH was utilized to adjust pH to 7.

2.2. Experimental setup and operating conditions:

A CG-AnMBR and a SG-AnMBR with the same effective working volume (3 L) were operated in parallel at 20 ºC in a temperature controlled room. The anaerobic sludge (MLSS = 22.34 ± 0.41 g/L, MLVSS = 17.41 ± 0.38 g/L, SVI = 98.5 mL/g, Mean particle size = 58 μm, Temperature = 21 ºC and pH = 7.5) was from the anaerobic digester of a wastewater treatment plant in Sydney and was acclimatized to synthetic

wastewater for 30 days until a stable treatment performance was reached. The two reactors were fed with identical acclimatized anaerobic sludge with MLSS of 20.50 ± 1.53 g/L in the reaction zone. A polyvinylidence (PVDF) hollow fiber membrane with a pore size of 0.22 μm and surface area of 0.06 m^2 was immersed in the mixed liquor at the settling zone of each reactor. A vacuum driven peristaltic pump was employed to feed influent into the upflow anaerobic granular sludge bioreactor (UAGB). The other suction pump was operated with an intermittent suction cycle of 8 min on and 2 min off to acquire permeate from the membrane module. The purpose of the on/off cycle was to relax membrane unit and prevent the membrane fouling. Porous polyester-urethane sponge cubes (dimensions: 2 mm × 2 mm × 2 mm), namely $S_{28–30/90}$ R (density of 28–30 kg/m^3 with 90 cells per 25 mm, Joyce Foam Products), were added into the UAGB of the SG-AnMBR together with the inoculated sludge, and sponge volume fraction was 10% working volume. The CG-AnMBR and SG-AnMBR were operated at a constant filtration rate of 5.3 L/m^2h with hydraulic retention time (HRT) of 12 h till membrane was fouled. Upflow velocity of 3.2 m/h was maintained using internal recirculation. The membrane fouling was indicated by development of the normalized TMP, which was recorded by a pressure transmitter. When TMP reached 30 kPa, operation was terminated. For the purpose of measuring membrane fouling resistance, hollow fibre membrane was taken out for chemical cleaning using the following three steps: 6 h in 0.4% sodium hydroxide, 6 h in 0.5% citric acid, and 6 h in 0.8% sodium hypochlorite.

2.3. Analytical methods

DOC of the sample was measured using a DOC analyzer (Analytikjena Multi N/C 2000). The equal amount of granular sludge was collected at 3 sampling port at different

heights of the UAGB (Port 1: 20 cm, Port 2: 40 cm and Port 3: 60 cm height from the bottom) and mixed for analysis, in order to represent the overall properties of granular sludge. The analysis of mixed liquor suspended solids (MLSS), mixed liquor volatile suspended solids (MLVSS), sludge volume index (SVI), settling velocity, zeta-potential were carried out according to Standard Methods [19]. Three sludge samples were taken each time and the average value was then calculated for measuring MLSS and granular biomass. The method suggested by Nguyen et al. [24] was used for determining attached biomass in sponge. Spectrophotometric method using spectroquant Cell Test (NOVA 60, Merck) was used to measure NH_4^+-N, NO_2^--N, NO_3^--N and PO_4^{3-}-P. PSD of granule sludge was determined by using the laser particle size analysis system Mastersizer Series 2000 (Malvern Instruments Ltd. UK) with a detection range of 0.02–2000 mm. D (0.1) (i.e. 10% of the volume distribution was below this value) was used to describe the colloidal and fine particle fractions. The sludge granules were also examined by Microscope BX41 (Olympus, Japan) using Image-Pro Plus software.

Membrane fouling resistance of the G-AnMBR was determined by the resistance-in-series model using the following two equations:

$$J = \Delta P/\mu R_T \quad (1)$$

$$R_T = R_M + R_C + R_P \quad (2)$$

Where J is the permeation flux ($m^3\ m^{-2}\ h^{-1}$); ΔP is the transmembrane pressure (Pa); μ is the dynamic viscosity of the permeate (Pa s); R_T is total resistance (m^{-1}); R_M is the intrinsic membrane resistance (m^{-1}); R_C is the cake layer resistance (m^{-1}); and R_P is the pore blocking resistance (m^{-1}). The method described by Deng et al. [20] was adopted

172 for the measurement protocol of filtration resistances including R_M, R_T, R_C and R_P,
173 respectively.
174
175 The extraction and analysis of EPS and SMP of the sludge sample, cake layer and
176 mixed liquor were performed using the methods suggested by Deng et al. [17].
177 Modified Lowry method (Sigma, Australia) and Anthrone-sulfuric acid method were
178 adopted for further determination protein (EPS_P and SMP_P) and polysaccharide (EPS_C
179 and SMP_C) concentrations of the extracted samples. The total SMP or EPS
180 concentration was calculated as the sum of the protein and polysaccharide. Foulants
181 attached on the surface of membrane was extracted based on the methods provided by
182 Johir et al. [21]. The extracted samples were further analysed using size exclusion liquid
183 chromatograph with organic carbon detector (LC-OCD), a TSK HW 50-(S) column and
184 a 0.028 mol/L phosphate buffer for the qualitative examination of the hydrophilic and
185 hydrophobic fractions of the membrane foulant.
186
187 Volatile fatty acids (VFAs), namely acetate acid, propionic acid, butyric acid,
188 isobutyric acid, iso-valeric acid and n-valeric acid were extracted using methyl-tert-
189 butyl ether (MTBE) for liquid-liquid extraction according to the methods reported by
190 Banel and Zygmunt [22]. Six VFAs were further quantified by gas chromatogram mass
191 spectrometry method (GC-MS TQ8040, Shimadzu, Japan) using an open tubular
192 analytical column (VF-WAXms, Agilent, US). An injection port equipped with a 1 mm
193 internal diameter (ID) liner operated in splitless mode (after 1 min, split ratio was 1:10)
194 was maintained at a temperature of 230 ˚C. Temperature program started at 50 ˚C and
195 was held for 5 min before ramping to 250 ˚C at 10 ˚C/min and was then held for 10 min.

196 Helium was a carrier gas operated at a flow rate of 2.05 mL/min. Electron impact ion
197 source was set at 230 ˚C while the injection port and transfer line temperatures were
198 held at 230˚C. Mass spectrometer (MS) was operated in a selected ion monitoring
199 (SIM) mode and in a full scan mode (m/z 15-550). Ions for detection of individual VFA
200 in SIM mode were selected using the mass spectra of standards generated in SCAN
201 mode. Biogas production was collected using a biogas sample bag and determined using
202 a liquor displacement device. Biogas composition including CH_4, CO_2, H_2 and N_2 is
203 determined using potable biogas analyzer (Biogas 5000, Geotech, UK).
204
205 **3. Results and discussion**
206 3.1. Organics and nutrient removal
207 Both AnMBRs achieved organics removal efficiency higher than 90%. More
208 specifically, the SG-AnMBR demonstrated slightly higher removals of DOC (92.4 ±
209 2.2%) and COD (93.7 ± 1.7%) when compared to those of the CG-AnMBR (90.1 ±
210 0.9% and 90.8 ±1.4 %, respectively). The relatively high organics removal efficiencies
211 could be attributed to the influent COD contained the majority of readily biodegradable
212 COD using glucose as the sole carbon source. The complete retention of all particulate
213 and colloidal matters by membrane also contributed to the high organics removal [23].
214 In general, total nitrogen (TN) and PO_4^{3-}-P removal in the CG-AnMBR was low, which
215 was found to be 15.0 ± 4.1% and 17.6 ± 6.2%, respectively. However, higher removal
216 efficiencies were observed in the SG-AnMBR (31.7 ± 6.8% for TN removal and 36.2 ±
217 7.9% for PO_4^{3-}-P removal), which is in line with the findings in Nguyen et al. [24]. The
218 results revealed that the addition of sponge could not only enhance the removal of
219 organic matter but also encourage nutrient removal in the G-AnMBR.

220

221 3.2. Granular sludge properties

222 3.2.1. Granular sludge

223 The successful implementation of anaerobic granular bioreactor technology relies
224 on its capacity to retain a dense granular sludge bed for efficient physical entrapment
225 and biodegradation of particulate and dissolved organic substances [25]. The CG-
226 AnMBR and SG-AnMBR have been operated for 25 and 55 days, respectively, when
227 TMP reached up to 30 kPa. As can be seen from Table 1, at the end of experimental
228 period, MLSS concentrations of granular sludge increased to 23.82 g/L and 21.30 g/L in
229 the SG-AnMBR and the CG-AnMBR, corresponding to the growth rate (ΔMLSS/Δt) of
230 0.060 g/L·d and 0.032 g/L·d, respectively. The higher biomass growth rate in the SG-
231 AnMBR indicated that the sponge addition encouraged the growth of retained sludge
232 agglomerates in the granular sludge bed. Furthermore, the SG-AnMBR also presented
233 higher MLVSS concentration with 19.10 g/L than that of the CG-AnMBR (16.59 g/L).
234 The biomass attached to the sponge was found at 1.28 ± 0.41 g/g sponge.

235

236 In addition, the granular sludge from the SG-AnMBR also presented superior
237 settling properties. At the end of the operation, granular sludge from the SG-AnMBR
238 had SVI of 20.1 mL/g with settling velocity varying from 17.5 to 32.5 m/h (Table 1).
239 Compared to the settling properties of the seed sludge, reduced SVI and increased
240 settling velocities indicated that the settling properties of granular sludge were enhanced
241 in the SG-AnMBR. On the other hand, granular sludge in the CG-AnMBR exhibited
242 higher SVI of 58.5 mL/g and lower settling velocity of 14.1-18.4 m/h than those of the
243 seed sludge, suggesting the sludge settleability was deteriorated. Zeta potential of the

244 granular sludge in the SG-AnMBR (-13.8 mV) was found higher than those of the CG-
245 AnMBR (-21.1 mV) and the seed sludge (-15.5 mV). With increased zeta potential, the
246 negative charge of the flocs could be neutralized and form large sludge aggregates with
247 better settling characteristics [8, 17]. Since the development of well settling granular
248 sludge requires selective washout of flocculent sludge with poor immobilization
249 properties, the complete retention of small and colloidal flocs in a G-AnMBR by
250 membrane barrier eliminated the hydraulic selection pressure required for granular
251 sludge with good settling capacities. In this case, the growth of dispersed sludge would
252 predominately take place, resulting in the bulking type of sludge formed in the CG-
253 AnMBR with poor settling properties [17]. However, sponge addition could somehow
254 improve granular sludge properties of the SG-AnMBR, and further alleviate the
255 deterioration of granular sludge settling properties.

256
257 **Table 1.**
258

259 3.2.2. Granules

260 Generally, it has been reported the formation of sludge aggregates on or over 500
261 μm could be considered as granules [26]. However, a few studies have regarded sludge
262 particles with 160 μm or less as granules [27-29]. Abbasi and Abbasi [12] suggested
263 that granules size could range from 100 μm to 5 mm while Zhang et al. [30] reported
264 average granule size increased from 111 μm to 264 μm from a hybrid anaerobic
265 granular system with internal hydraulic circulation. Thus, in this study, bioparticles over
266 100 μm was considered as granules since synthetic domestic wastewater with low
267 organic loading rate of 0.53-0.59 kg COD/m^3·d was used as the feed and relatively short
268 operation time was adopted. As compared to the seed sludge, one-way shift to fine

269 particles was observed in the CG-AnMBR while bigger size granules tended to form in
270 the SG-AnMBR (Fig. 1). Based on the PSD of the granular sludge, the SG-AnMBR
271 presented granules with increased diameter, compared to those of the CG-AnMBR. Fig.
272 1 shows that the percentage of granules (>100 μm) was approximately 84% of the total
273 granular sludge in the SG-AnMBR, which was almost two times to the corresponding
274 value obtained from the CG-AnMBR (42.5%). As membrane functioned as an absolute
275 barrier in the CG-AnMBR, fine sludge particles (<100 μm), such as colloidal flocs,
276 macromolecules of SMP and non-settling particles, could not be effectively discharged
277 and rather accumulated in the CG-AnMBR, presenting lower percentage of granules. In
278 contrast, sponge addition could assist granular growth by immobilizing fine particles on
279 or inside the sponge pores, contributing to larger fraction of granules.
280
281 **Fig. 1.**
282
283 Apart from the complete retention of fine sludge particles, granules breakage could
284 be another explanation for the lower amount of granules in the CG-AnMBR. Normally,
285 EPS in the sludge plays a vital role in the synthesis of anaerobic granules, and is crucial
286 for integrating cells into granules and maintaining intact structure of the granules. At the
287 end of experiment, both protein and polysaccharides amounts of EPS decreased by
288 81.1% and 77.1% in the CG-AnMBR, as compared to the seed sludge EPS (EPS_p and
289 EPS_c: 20.2 and 6.9 mg/g VSS), respectively. Therefore, the significant decrease in EPS
290 amount might indicate scattered, looser and weaker structures of granules (Fig. S1 in
291 supplementary information), meaning granule fragmentation and decrease in particle
292 size, as well as SMP increase in the mixed liquor [8]. On the contrary, the stable EPS

293 production in the SG-AnMBR was observed with the average values of 28.8 and 8.6
294 mg/g VSS for EPS_P and EPS_C, respectively. Therefore, the higher contents of EPS
295 promoted granule growth in the SG-AnMBR. Additionally, the amount of SMP from
296 the CG-AnMBR sludge granules (Protein: 25.1 mg/g VSS, polysaccharide: 8.2 mg/g
297 VSS) were found approximately 7 times higher than those from the SG-AnMBR (3.2
298 mg/g VSS, and 1.1 mg/g VSS). Much lower SMP values of the SG-AnMBR confirmed
299 the majority of proteins and polysaccharides existed as the part of the anaerobic
300 granules. As a result, the sponge addition had profound impacts on the EPS production
301 of the anaerobic granules, as well as the granules abundance, structure and stability.
302
303 3.3. Membrane fouling behaviour
304 3.3.1. TMP profile
305 Fig. 2 showed the membrane fouling profile indicated by TMP development in two
306 G-AnMBRs. Both systems showed significant differences in TMP profiles. As for the
307 CG-AnMBR, the increase in TMP with time was characterized by a gradual rise at 0.3
308 kPa/d from day 1 to day 15, and then a rapid increase at 2.4 kPa/d till membrane was
309 severely fouled on day 25. On the other hand, TMP in the SG-AnMBR was maintained
310 well below 6 kPa within the first 25 days of operation and reached 30 kPa on day 55,
311 indicating a relatively lower fouling rate of 0.5 kPa/d compared to the averaged 1.2
312 kPa/d for the CG-AnMBR. The results revealed that the sponge addition could greatly
313 reduce fouling rate and improve the filtration performance of the G-AnMBR
314
315 **Fig. 2.**
316

317 3.3.2. SMP and EPS of the mixed liquor in settling zone

318 Membrane fouling was often attributed to the accumulation of organics in or on the
319 membrane in the form of EPS and SMP [31]. Studies have reported that EPS clog the
320 membrane pores, promoting the formation of a strongly attached fouling layer on the
321 membrane surface while SMP can be absorbed onto the membrane surface, thereby
322 blocking its pores and forming a gel layer acting as a barrier for permeate flux during
323 filtration [20, 32]. Since the membrane was submerged in the mixed liquor of the G-
324 AnMBR settling zone, SMP and EPS of the mixed liquor in both G-AnMBRs were
325 analysed in order to explain the relationship between the mixed liquor properties and
326 membrane fouling. As shown in Fig. 3, averaged SMP concentration in the CG-AnMBR
327 was 47.3 ± 7.6 mg/L, which is almost three times higher than the value obtained in the
328 SG-AnMBR (15.9 ± 3.5 mg/L). The significantly higher SMP amount in the CG-
329 AnMBR was due to the release of biopolymeric susbstances to the mixed liquor as a
330 result of granule and floc breakage and cell lysis [33]. This observation was further
331 supported with particle size analysis, and EPS analysis of the granular sludge in Section
332 3.2. The bound EPS in the sludge could also be dissolved/ hydrolyzed into small
333 fractions by bacterial hydrolysis [31]. Their subsequent dissolution into the water phase
334 could result in more SMP release from microbial aggregates into the mixed liquor [8].
335
336 **Fig. 3.**
337
338 EPS concentrations of both systems remained increasing (Fig. 3) with the MLSS
339 build-up in the mixed liquor. The MLSS concentrations in both G-AnMBRs increased
340 gradually throughout the experimental period. At the end of experiment, the MLSS

341 concentration in the CG-AnMBR reached up to 770.2 mg/L, which was nearly 3 times
342 higher than that of the SG-AnMBR (260.2 mg/L). The build-up of MLSS in the mixed
343 liquor was mainly due to the membrane's complete retention of small and colloidal
344 flocs that would be otherwise selectively washed out from the system. The EPS
345 concentration averaged at 17.0 ± 6.2 mg/L (SG-AnMBR) and 24.5 ± 11.0 mg/L (CG-
346 AnMBR), and peaked at 24.5 mg/L (SG-AnMBR) and 39.3 (CG-AnMBR) when TMP
347 reached 30 kPa. In the SG-AnMBR, sponge addition could help to limit the suspended
348 growth [17], thus significantly reducing SMP and EPS concentrations in the mixed
349 liquor by the means of adsorption onto the sponge and biodegradation by the attached
350 biomass of the sponge. In addition, well-balanced granular and attached growth
351 provided a sound environment for granules growth in the SG-AnMBR. Thus, the
352 biodegradation of organics occurs mainly within the granules and attached biomass of
353 the sponge, limiting the dispersed growth of light flocs. Colloidal particles coming from
354 the influent solids could therefore be physically adsorbed and retained in the thick and
355 dense granule bed, preventing their impact on the fouling [10].
356
357 3.3.3. Analysis of fouling resistance, cake layer and foulants
358 The fouling resistance was calculated according to the resistance-in-series model
359 and the results are shown in Table 2. The R_T of SG-AnMBR and CG-AnMBR were 9.7
360 $\times$ 10^{13} m^{-1} and 19.7 $\times$ 10^{13} m^{-1}, respectively, indicating sponge addition into SG-
361 AnMBR reduced the R_T by 50.7%., compared to the CG-AnMBR. Higher R_P was also
362 found for the CG-AnMBR compared to the SG-AnMBR, corresponding to 9.5×10^{12} m^{-1}
363 and 4.6×10^{12} m^{-1}, respectively. R_C of the CG-AnMBR (18.7×10^{13} m^{-1}) accounted for
364 94.9% of R_T, whereas the SG-AnMBR had much lower R_C at 9.2×10^{13} m^{-1},

365 corresponding to 94.8% of R_T. The resistance caused by R_C presented dominant
366 proportion of total resistance for both systems. Hence, minimizing the cake formation is
367 of great importance to lower the fouling propensity of the G-AnMBR
368
369 **Table 2.**
370
371 Contrarily, pore clogging, due to particles or colloids with equal or smaller size
372 than the membrane pores, contributed to small portion of fouling resistance. The results
373 were consistent with the findings of Liu et al. [34] in which sludge cake formation was
374 the main mechanism of membrane fouling in the G-AnMBR. Jeison et al. [35, 36] also
375 reported that TMP and flux was mainly governed by cake formation. The higher cake
376 layer resistance in the CG-AnMBR could be ascribed to higher MLSS concentration in
377 the mixed liquor where membrane was immersed. Assisted by sponge, the SG-AnMBR
378 demonstrated the efficient solids entrapment of the dense granular sludge bed and
379 contained much reduced MLSS of the mixed liquor. Lin et al. [37] identified that the
380 cake formation rate was significantly affected by colloidal and fine particle size D (0.1)
381 of PSD. D (0.1) of the CG-AnMBR was 30.1 μm, which was much smaller than those
382 of the SG-AnMBR (62.5 μm). Considering the denser structure and reduced back
383 transport velocity of the fine flocs, Liu et al. [34] suggested that the greater amount of
384 fine particles in the CG-AnMBR are more likely to deposit on the surface of membrane,
385 which in turn facilitates a cake layer denser than that with larger particles. Therefore,
386 the results proved the sponge addition could greatly alleviate membrane fouling mainly
387 by reducing the cake layer formation and pore clogging.
388

389 The compositions of bound EPS and SMP of the cake layer from both reactors
390 were also analysed and compared. As shown in Table 2, sponge addition could
391 efficiently reduce EPS_P and SMP production in the cake layer of the SG-AnMBR.
392 Higher concentration of EPS_P (12.1 mg/g cake layer) was found in the CG-AnMBR
393 than that in the SG-AnMBR (10.7 mg/g cake layer), while minor difference could be
394 observed on EPS_C of the cake layer from both G-AnMBRs. The CG-AnMBR
395 demonstrated higher concentrations of SMP_P and SMP_C in the cake layer (8.2 and 4.1
396 mg/g cake layer, respectively) compared to the SG-AnMBR (5.6 and 2.5 mg/g cake
397 layer, respectively). These results implied EPS_P, SMP (including SMPp and SMPc) on
398 the surface of the membrane were responsible for the higher R_C in the CG-AnMBR. At
399 relatively high TMP, more EPS_P, SMP_P, and SMP_C could be deposited onto the
400 membrane surface due to the high drag force from the permeate pump. Furthermore, the
401 endogenous decay or cell lysis at the bottom layer could result in the release of more
402 EPS_P and SMP due to more sludge cake accumulated on the membrane surface [20].
403
404 LC-OCD provides important information regarding the fraction of organic matter
405 in foulants by dividing the total organics into hydrophobic and hydrophilic groups. The
406 hydrophilic fraction can be further subdivided into biopolymers, humic substances,
407 building blocks, low molecular weight (LMW) acids and LMW neutrals and acids. As
408 can be seen from Table 3, hydrophilic organics mainly contributed to membrane
409 fouling, in which biopolymer was regarded one of the major foulants [21]. The value of
410 biopolymers for the CG-AnMBR was found twice higher (34.6%) as compared to that
411 for the SG-AnMBR (17.1%). The higher biopolymer concentrations in the CG-AnMBR
412 indicated more hydrophilic layers built up on the membrane surface [38]. Furthermore,

413 bridging between inorganic compounds and deposited biopolymers could encourage the
414 formation of more compact and dense fouling layer, leading to sever fouling [39].
415 Greater amount of building blocks (17.0% vs. 13.9%) and LMW neutrals and acids
416 (35.1% vs. 31.2%) were also found in the CG-AnMBR compared to the SG-AnMBR.
417 Aryal et al. [40] reported that building blocks and LMW neutrals and acids were vital
418 factors causing fouling and enhancing the formation of biopolymers on the surface of
419 the membrane possibly through their assemblage. Nevertheless, the CG-AnMBR
420 exhibited lower humic substances (10.5%) than the SG-AnMBR (31.3%). Since the
421 building blocks were the breakup of humic substances, lower fraction of humic
422 substances might be related to the higher amount of building blocks in foulants of the
423 CG-AnMBR [38].

424
425 **Table 3.**
426

427 3.4. VFA and biogas production

428 VFA serves as the most important process indicator for biogas production from G-
429 AnMBRs not only because it can significantly influence pH value of the reactor but also
430 due to the fact that it is the vital intermediary substrate for the methane generation [41].
431 Approximately 75% of methane yield comes from decarboxylation of acetic acid (main
432 component of VFA) and the rest 25% is from CO_2 and H_2 [42]. If existing in high
433 concentrations, VFA can also cause significant pH drop and pose enormous stress on
434 sensitive methane-producing bacteria, thus ultimately resulting in G-AnMBRs reactor
435 acidification and low biogas production [43-46]. In this study, seven types of VFAs
436 including acetic (C_2), propionic (C_3), iso-butyric (i-C_4), n-butyric (n-C_4), iso-valeric
437 acid (i-C_5), n-valeric (C_5) and caproic acid (C_6) were monitored. The SG-AnMBR

exhibited much lower level of acetic acid with the average value of 3.5 ± 0.8 mg/L, while other acids were at undetectable level (Table 4). The results revealed that there was no VFA accumulation in the SG-AnMBR, and reactor acidification was rarely encountered over the operation time. Therefore, the sponge could help to maintain a well-functioning granular sludge bed and efficient VFA degradation.

In contrast, the CG-AnMBR demonstrated much higher VFA concentrations with an average value of 20.2 ± 2.7 mg/L (5.8 times higher than that of the CG-AnMBR). VFA accumulation was mainly attributed to the existence of acetic acid (67.4 ± 7.7%) in the mixed liquor. C_3, i-C_4, n-C_4, i-C_5 and n-C_5 were also detected in the CG-AnMBR. The accumulation of intermediate products VFA might be related to the VFA release as a result of granule disintegration or deteriorated methanogenic process. The stability of methanogensis process is the key to the efficient biogas production. Since methanogens are very sensitive to environmental factor (oxidation/reduction potential (ORP), pH, etc), any variations in the operating conditions may cause inhibition for biogas production. Average pH values were found at 7.3 ± 0.3 and 6.9 ± 0.2 in the SG-AnMBR and CG-AnMBR, respectively, even though pH was not controlled. In the CG-AnMBR, the higher VFAs concentrations were accompanied by lower values of pH [47]. The changes of the ORP were also recorded. The ORP value in the SG-AnMBR was -318.4 ± 8.9 mV, which was 58.9 ± 8.9 mV lower than that in the CG-AnMBR on average. Lower ORP favoured the survival and growth of methanogens, therefore enhancing the transformation of VFAs into CH_4 [29].

Table 4.

462

463 The SG-AnMBR produced more biogas (486 ± 12 mL/d) than the CG-AnMBR
464 (456 ± 9 mL/d) with similar methane and carbon dioxide composition in the biogas
465 (69.8 and 26.5%, 67.5 and 28.1%, respectively) (Table 5). Very small amount of H_2
466 with 5 - 12 ppm was also detected in the biogas from both reactors. The CG-AnMBR
467 achieved methane yield at 133.3 ± 5.3 mL $CH_{4\ (STP)}$/g $COD_{removed}$, volume of methane
468 produced at and 0 °C Standard Temperature and 1 atm Pressure). While the SG-
469 AnMBR had higher methane yield of 156.3 ± 5.8 mL $CH_{4\ (STP)}$/g $COD_{removed}$.

470

471 **Table 5.**

472

473 The methane yield from the SG-AnMBR represented around 50% of the optimal
474 theoretical value of 318 mL $CH_{4\ (STP)}$/g $COD_{removed}$. As it is reported that methane loss
475 in the liquid phase from the anaerobic MBR could be as much as 30% and 50% at 35 °C
476 and 15 °C, respectively [48], nearly half of degraded COD might convert to dissolved
477 methane and lost. Considering the economic and environmental impacts, methane
478 leakages have to be paid much attention to and minimized [49, 50]. The development of
479 feasible and effective recovery process for dissolved methane is highly desired for the
480 optimization of bioenergy recovery and minimization of greenhouse gas emissions to
481 the atmosphere. The available recovery processes include biological oxidation of
482 dissolved methane using down-flow hanging sponge reactor [51], removal of residual
483 dissolved methane using degassing membrane [52] and post-treatment aeration to strip
484 of AnMBR effluent [53].

485

486 **4. Conclusions**

This study showed that the sponge addition into G-AnMBR could not only improve organics and nutrient removal, but also retain superior granular sludge properties and enhance methane yield. In addition, the SG-AnMBR exhibited prolonged operation time due to effective fouling mitigation. Assisted by sponge, the SG-AnMBR showed lower SMP and EPS levels in settling zone mixed liquor, less EPS_P and SMP production in the cake layer as well as much lower cake layer and pore clogging resistance compared to those of the CG-AnMBR. Fouling resistance analysis revealed that sponge addition could reduce the R_T by 50.7% via decreasing both cake layer and pore logging resistance. Furthermore, LC-OCD analysis confirmed that lower biopolymers, LMW neutrals and acids and building blocks were presented in the SG-AnMBR foulant. Further research on microbiological analysis is needed to look into differences in microbiological population or differences in the evolution of microbiological population in both SG-AnMBR and CG-AnMBR. This work offers a useful performance enhancement and fouling control strategy that a certain sponge volume could be added into the UAGB during G-AnMBR process.

References

[1] J. Ferrer, R. Pretel, F. Duran, J.B. Gimenez, A. Robles, M.V. Ruano, J. Serralta, J. Ribes, A. Seco, Design methodology for submerged anaerobic membrane bioreactors (AnMBR): A case study, Sep. Purif. Technol. 141 (2015) 378-386.

[2] P. Kaparaju, J. Rintala, Mitigation of greenhouse gas emissions by adopting anaerobic digestion technology on dairy, sow and pig farms in Finland, Renew. Energ. 36 (2011) 31-41.

[3] M. Herrera-Robledo, D.M. Cid-Leon, J.M. Morgan-Sagastume, A. Noyola, Biofouling in an anaerobic membrane bioreactor treating municipal sewage, Sep. Purif. Technol. 81 (2011) 49-55.

[4] M. Andalib, E. Elbeshbishy, N. Mustafa, H. Hafez, G. Nakhla, J. Zhu, Performance of an anaerobic fluidized bed bioreactor (AnFBR) for digestion of primary municipal wastewater treatment biosolids and bioethanol thin stillage, Renew. Energ. 71 (2014) 276-285.

[5] C. Chen, W.S. Guo, H.H. Ngo, Advances in granular growth anaerobic membrane bioreactor (G-AnMBR) for low strength wastewater treatment, Journal of Energy and Environmental Sustainability 1 (2016a) 77-83.

[6] N. Massalha, A. Brenner, C. Sheindorf, I. Sabbah, Application of immobilized and granular dried anaerobic biomass for stabilizing and increasing anaerobic bio-systems tolerance for high organic loads and phenol shocks, Bioresour. Technol. 197 (2015) 106-112.

[7] P. Gupta, T.R. Sreekrishnan, S.Z. Ahammad, Role of sludge volume index in anaerobic sludge granulation in a hybrid anaerobic reactor, Chem. Eng. J. 283(2016) 338-350.

[8] H. Ozgun, J.B. Gimenez, M.E. Ersahin, Y. Tao, H. Spanjers, J.B. van Lier, Impact of membrane addition for effluent extraction on the performance and sludge characteristics of upflow anaerobic sludge blanket reactors treating municipal wastewater, J. Membr. Sci. 479 (2015) 95-104.

[9] I.M. Garcia, M. Mokosch, A. Soares, M. Pidou, P. Le-Clech, S.J. Judd, E.J. McAdam, B. Jefferson, Impact of membrane configuration on fouling in anaerobic membrane bioreactors, J. Membr. Sci. 382 (2011) 41-49.

534 [10] I.M. Garcia, M. Mokosch, A. Soares, M. Pidou, B. Jefferson, Impact of reactor
535 configuration on the performance of anaerobic MBRs: Treatment of settled sewage
536 in temperature climates, Water Res. 47 (2013) 4853-4860.
537 [11] H. Ozgun, R.K. Dereli, M.E. Ersahin, C. Kinaci, H. Spanjers, J.B. van Lier, A
538 review of anaerobic membrane bioreactors for municipal wastewater treatment:
539 Integration options, limitations and expectations, Sep. Purif. Technol. 118 (2013)
540 89-104.
541 [12] T. Abbasi, S.A. Abbasi, Formation and impact of granules in fostering clean energy
542 production and wastewater treatment in upflow anaerobic sludge blanket (UASB)
543 reactors, Renew. Sustainable Energy Rev. 16 (2012) 1696-1708.
544 [13] X.G. Chen, P. Zheng, M. Qaisar, C.J. Tang, Dynamic behaviour and concentration
545 distribution of granular sludge in a super-high-rate spiral anaerobic bioreactor,
546 Bioresour. Technol. 111 (2012) 134-140.
547 [14] J. Wu, J.B. Zhang, S. Poncin, H.Z. Li, J.K. Jiang, Z.U. Rehman, Effects of rising
548 biogas bubbles on the hydrodynamic shear conditions around anaerobic granule,
549 Chem. Eng. J. 273 (2015) 111-119.
550 [15] W.S. Guo, H.H. Ngo, F. Dharmawan, C.G. Palmer, Roles of polyurethane foam in
551 aerobic moving and fixed bed bioreactors, Bioresour. Technol. 101 (2010) 1435-
552 1439.
553 [16] W.S. Guo, H.H. Ngo, S. Vigneswaran, W. Xing, P. Goteti, A novel sponge
554 submerged membrane bioreactor (SSMBR) for wastewater treatment and reuse,
555 Sep. Purif. Technol. 43 (2008) 273-285.
556 [17] L. Deng, W.S. Guo, H.H. Ngo, J. Zhang, S. Liang, S. Xia, Z. Zhang, J. Li, A
557 comparison study on membrane fouling in a sponge-submerged membrane

558 bioreactor and a conventional membrane bioreactor, Bioresour. Technol. 165 (2014)
559 69-74.
560 [18] W.S. Guo, H.H. Ngo, C.G. Palmer, W. Xing, A.Y.J. Hu, A. Listowski, Roles of
561 sponge sizes and membrane types in a single stage sponge-submerged membrane
562 bioreactor for improving nutrient removal from wastewater for reuse, Desalination
563 249 (2009) 672-676.
564 [19] APHA, AWWA, WEF, Standard Methods for the Examination of Water and
565 Wastewater, 20th ed. American Public Health Association, Washington, DC, 1998.
566 [20] L.J. Deng, W.S. Guo, H.H. Ngo, M.F.R. Zuthi, J. Zhang, S. Liang, J.X. Li, J. Wang,
567 X.B. Zhang, Membrane fouling reduction and improvement of sludge
568 characteristics by bioflocculant addition in submerged membrane bioreactor, Sep.
569 Purif. Technol. 156 (2015) 450-458.
570 [21] M.A.H. Johir, S. Vigneswaran, A. Sathasivan, J. Kandasamy, C.Y. Chang, Effects
571 of organic loading rate on organic matter and foulant characteristics in membrane
572 bio-reactor, Bioresour. Technol. 113 (2012) 154-160.
573 [22] A. Banel, B. Zygmunt, Application of gas chromatography-mass spectrometry
574 preceded by solvent extraction to determine volatile fatty acids in wastewater of
575 municipal, animal farm and landfill origin, Water Sci. Technol. 63 (2011) 590-597.
576 [23] D. Martinez-Sosa, B. Helmreich, T. Netter, S. Paris, F. Bischof, Anaerobic
577 submerged membrane bioreactor (AnMBR) for municipal wastewater treatment
578 under mesophilic and psychrophilic temperature conditions, Bioresour. Technol.
579 102 (2011) 10377–10385.

580 [24] T.T. Nguyen, H.H. Ngo, W.S. Guo, S. Phuntsho, J.X. Li, A new sponge tray
581 bioreactor in primary treated sewage effluent treatment, Bioresour. Technol. 102
582 (2011) 5444-5447.
583 [25] L. Seghezzo, G. Zeeman, J.B. van Lier, H.V.M. Hamelers, G. Lettinga, A review:
584 the anaerobic treatment of sewage in UASB and EGSB reactors, Bioresour.
585 Technol. 65 (1998) 175–190.
586 [26] P. Bhunia, M.M. Ghangrekar, Required minimum granule size in UASB reactor
587 and characteristics variation with size, Bioresour. Technol. 98 (2007) 994-999.
588 [27] H.H. Chou, J.S. Huang, Comparative granule characteristics and biokinetics of
589 sucrose fed and phenol fed UASB reactors, Chemosphere 59 (2005) 107–116.
590 [28] A. Pevere, G. Guibaud, van E. Hullebusch, P. Lens, M. Baudu, Viscosity evolution
591 of anaerobic granular sludge, Biochem. Eng. J. 27 (2006) 315–322.
592 [29] Y.B. Zhang, X.L. An, X. Quan, Enhancement of sludge granulation in a zero
593 valence iron packed anaerobic reactor with a hydraulic circulation, Process
594 Biochem. 46 (2011) 471-476.
595 [30] Y.B. Zhang, Y.G. Ma, X. Quan, Y.W. Jing, S.C. D, Rapid startup of a hybrid
596 UASB-AFF reactor using bi-circulation, Chem. Eng. J. 155 (2009) 266-271.
597 [31] W.S. Guo, H.H. Ngo, J.X. Li, A mini-review on membrane fouling, Bioresour.
598 Technol. 122 (2012) 27-34.
599 [32] Y.H. Xiong, M. Harb, P.Y. Hong, Characterization of biofoulants illustrates
600 different membrane fouling mechanisms for aerobic and anaerobic membrane
601 bioreactors, Sep. Purif. Technol. 157 (2016) 192–202.
602 [33] C. Kunacheva Y.N.A. Soh, A.P. Trzcinski, D.C. Stuckey, Soluble microbial
603 products (SMPs) in the effluent from a submerged anaerobic membrane bioreactor

(SAMBR) under different HRTs and transient loading conditions, Chem. Eng. J. 311 (2017) 72–81.

[34] Y. Liu, H.N. Liu, L. Cui, K.S. Zhang, The ratio of food-to-microorganism (F/M) on membrane fouling of anaerobic membrane bioreactors treating low-strength wastewater. Desalination 297 (2012) 97-103.

[35] D. Jeison, B. Kremer, J.B. van Lier, Application of membrane enhanced biomass retention to the anaerobic treatment of acidified wastewaters under extreme saline conditions, Sep. Purif. Technol. 64 (2008) 198-205.

[36] D. Jeison, J.B. van Lier, Cake formation and consolidation: main factors governing the applicable flux in anaerobic submerged membrane bioreactors (AnSMBR) treating acidified wastewaters, Sep. Purif. Technol. 56 (2007) 71–78.

[37] H.J. Lin, K. Xie, B. Mahendran, D.M. Bagley, K.T. Leung, S.N. Liss, B.Q. Liao, Factors affecting sludge cake formation in a submerged anaerobic membrane bioreactor, J. Membr. Sci. 361 (2010) 126–134.

[38] S. Hong, R. Aryal, S. Vigneswaran, M.A.H Johir, J. Kandasamy, Influence of hydraulic retention time on the nature of foulant organics in a high rate membrane bioreactor, Desalination 287 (2012) 116-122.

[39] Y. An, Z.W. Wang, Z.C. Wu, D.H. Yang, Q. Zhou, Characterization of membrane foulants in an anaerobic non-woven fabric membrane bioreactor for municipal wastewater treatment, Chem. Eng. J. 155 (2009) 709-715.

[40] R. Aryal, J. Legegue, S. Vigneswaran, J. Kandasamy, M. Heran, A. Grasmick, Identification and characterisation of biofilm formed in membrane bioreactor, Sep. Purif. Technol. 67 (1) (2009) 86–94.

627 [41] M. Gulhane, P. Pandit, A. Khardenavis, D. Singh, H. Purohit, Study of microbial
628 community plasticity for anaerobic digestion of vegetable waste in Anaerobic
629 Baffled Reactor, Renew. Energ. 101 (2017) 59-66.
630 [42] P.L. McCarty, D.P. Smith, Anaerobic wastewater treatment, Environ. Sci. Technol.
631 20 (1986) 1200-1226.
632 [43] K.P. Roberts, S. Heaven, C.J. Banks, Quantification of methane losses from the
633 acclimatisation of anaerobic digestion to marine salt concentrations, Renew. Energ.
634 86 (2016) 497-506.
635 [44] C. Chen, W.S. Guo, H.H. Ngo, D.J. Lee, K.L. Tung, P.K. Jin, J. Wang, Y. Wu,
636 Challenges in biogas production from anaerobic membrane bioreactors, Renew.
637 Energ. 98 (2016b) 120-134.
638 [45] A. Jeihanipour, S. Aslanzadeh, K. Rajendran, G. Balasubramanian, M.J.
639 Taherzadeh, High-rate biogas production from waste textiles using a two-stage
640 process, Renew. Energ. 52 (2013) 128-135.
641 [46] X.W. Peng, I.A. Nges, J. Liu, Improving methane production from wheat straw by
642 digestate liquor recirculation in continuous stirred tank processes, Renew. Energ.
643 85 (2016) 12-18.
644 [47] Q.G. Zhang, J.J. Hu, D.J. Lee, Biogas from anaerobic digestion processes: Research
645 updates, Renew. Energ. 98 (2016) 108-119.
646 [48] A.L. Smith, L.B. Stadler, N.G. Love, S.J. Skerlos, L. Raskin, Perspectives on
647 anaerobic membrane bioreactor treatment of domestic wastewater: A critical review,
648 Bioresour. Technol. 122 (2012) 149-159.
649 [49] D.P. Chynoweth, J.M. Owens, R. Legrand, Renewable methane from anaerobic
650 digestion of biomass, Renew. Energ. 22 (2001) 1-8.

651 [50] I. Karakurt, G. Aydin, K. Aydiner, Sources and mitigation of methane emissions by
652 sectors: A critical review, Renew. Energ. 39 (2012) 40-48.
653 [51] M. Hatamoto, T. Miyauchi, T. Kindaichi, N. Ozaki, A. Ohashi, Dissolved methane
654 oxidation and competition for oxygen in downflow hanging sponge reactor for
655 post-treatment of anaerobic wastewater treatment, Bioresour. Technol. 102 (2011)
656 10299-10304.
657 [52] R. Moreno, M.I. San-Martin, A. Moran, Domestic wastewater treatment in parallel
658 with methane production in a microbial electrolysis cell, Renew. Energ. 93 (2016)
659 442-448.
660 [53] P.L. McCarty, J. Bae, J. Kim, Domestic wastewater treatment as a net energy
661 producer—can this be achieved? Environ. Sci. Technol. 45 (2011) 7100-7106.
662

Table titles

Table 1.

Summary of sludge characteristics of seed sludge and granular sludge in G-AnMBRs.

Sludge properties	Seed sludge	Granular sludge (CG-AnMBR)	Granular Sludge (SG-AnMBR)
MLSS (g/L)	20.50 ± 1.53	21.30 ± 0.91	23.82 ± 1.83
MLVSS (g/L)	16.21 ± 1.85	16.59 ± 1.28	19.10 ± 1.11
Zeta-potential (mV)	-15.5 ± 3.5	-21.1 ± 2.5	-13.8 ± 1.8
SVI (mL/g)	38.8 ± 4.8	58.5 ± 5.1	20.1 ± 4.2
Settling velocity (m/h)	15.51 - 25.42	14.1-18.4	17.5 - 32.5

Table 2.

Fouling resistance and cake layer analysis for both G-AnMBRs.

		CG-AnMBR	SG-AnMBR
Fouling resistance (m^{-1})	R_T [a]	19.7×10^{13}	9.7×10^{13}
	R_C [b]	18.7×10^{13}	9.2×10^{13}
	R_P [c]	9.5×10^{12}	4.6×10^{12}
	R_M [d]	5.7×10^{11}	5.1×10^{11}
SMP and EPS in the cake layer (mg/g cake layer)	EPS_P [e]	12.1	10.7
	EPS_C [f]	3.6	3.4
	SMP_P [g]	8.2	5.6
	SMP_C [h]	4.1	2.5

[a] R_T = total fouling resistance, [b] R_C = cake layer resistance, [c] R_P = pore blocking resistance, [d] R_M = clean membrane resistance, [e] EPS_P = protein concentration of extracellular polymeric substances, [f] EPS_C = polysaccharides concentration of extracellular polymeric substances, [g] SMP_P = protein concentration of soluble microbial products, [h] SMP_C = polysaccharides concentration of soluble microbial products.

Table 3.

Organic fractions of membrane foulants based on LC-OCD analysis.

Operating conditions		DOC [a] dissolved	HOC [b] Hydrophobic	CDOC [c] Hydrophilic	Biopolymers	Humic substances	Building blocks	LMW neutrals and acids
Description	G-AnMBRs	ppb-C, (% DOC)	ppb-C (% DOC)		ppb-C (% DOC)			
Foulant	SG-AnMBR	5360	508	4852	918	1675	743	1516
		(100%)	(9.5%)	(90.5%)	(17.1%)	(31.3%)	(13.9%)	(31.2%)
Foulant	CG-AnMBR	5373	152	5221	1857	565	915	1884
		(100%)	(2.8%)	(97.2%)	(34.6%)	(10.5%)	(17.0%)	(35.1%)

[a] DOC = dissolved organic carbon, [b] HOC = hydrophobic organic carbon , [c] CDOC = chromatographic dissolved organic carbon.

Table 4.

VFAs concentrations in the CG-AnMBR and the SG-AnMBR.

VFA	CG-AnMBR		SG-AnMBR	
	Concentration (mg/L)	Fraction of VFA (%)	Concentration (mg/L)	Fraction of VFA (%)
C_2 [a]	13.6 ± 2.6	67.4 ± 7.7	3.5 ± 0.8	100
C_3 [b]	1.4 ± 0.9	6.9 ± 4.8	0	0
i-C_4 [c]	1.0 ± 0.6	5.2 ± 3.5	0	0
n-C_4 [d]	0.9 ± 0.7	4.6 ± 3.7	0	0
i-C_5 [e]	1.1 ± 0.8	5.6 ± 4.4	0	0
n-C_5 [f]	2.2 ± 2.2	10.3 ± 9.3	0	0
C_6 [g]	0	0	0	0
V_T [h]	20.2 ± 2.7	100	3.5 ± 0.8	100

[a] C_2=acetic acid, [b] C_3=propionic acid, [c] i-C_4=iso-butyric acid, [d] C_4=butyric acid, [e] i-C_5=iso-valeric acid, [f] C_5=valeric acid, [g] C_6= caproic acid, [h] V_T=total volatile fatty acids.

Table 5.

Biogas yield from the CG-AnMBR and the SG-AnMBR.

Parameter	SG-AnMBR	CG-AnMBR
Biogas volume (mL/d)	486 ± 12	456 ± 9 mL/d
Methane yield ($mL\ CH_4/g\ COD_{removed}$)	156.3 ± 5.8 at STP [a]	133.3 ± 5.3 at STP
Methane (%)	69.8 ± 4.2	67.5 ±4.8
Carbon dioxide (%)	26.5 ± 4.8	28.1 ± 4.5
Hydrogen (ppm)	9.2 ± 2.8	8.1 ± 3.1

[a] STP = vo.lume of methane produced at and 0 °C Standard Temperature and 1 atm Pressure.

Figures captions

Fig. 1. Particle size distribution of seed sludge, and granular sludge for both G-AnMBRs.

Fig. 2. TMP profile of the CG-AnMBR and the SG-AnMBR over the experimental period.

Fig. 3. Variations of EPS and SMP concentrations in the settling zone of G-AnMBR at designated TMPs.

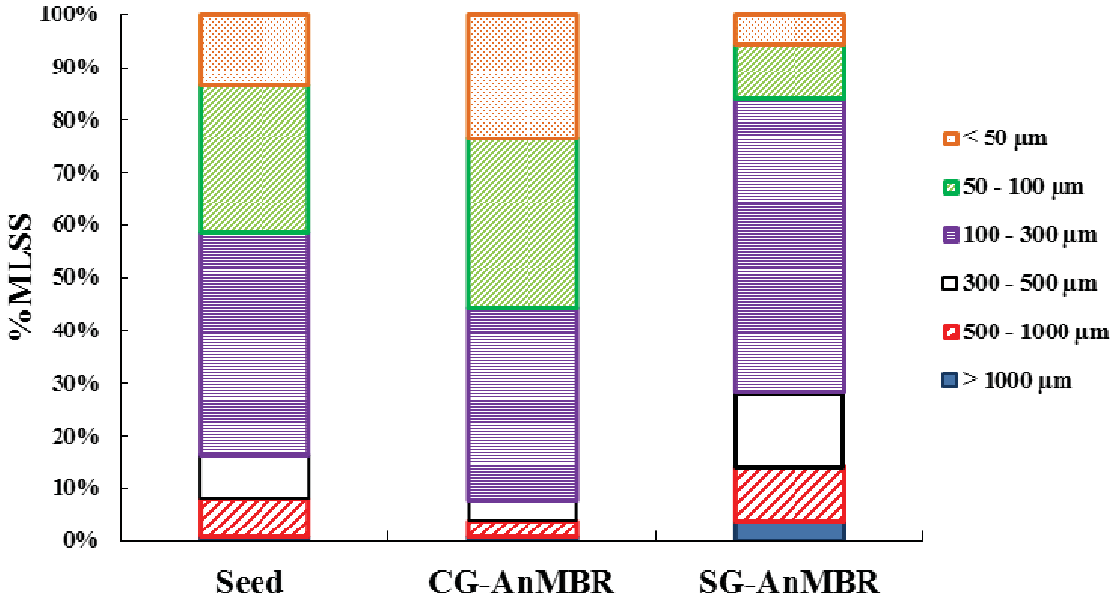

Fig. 1.

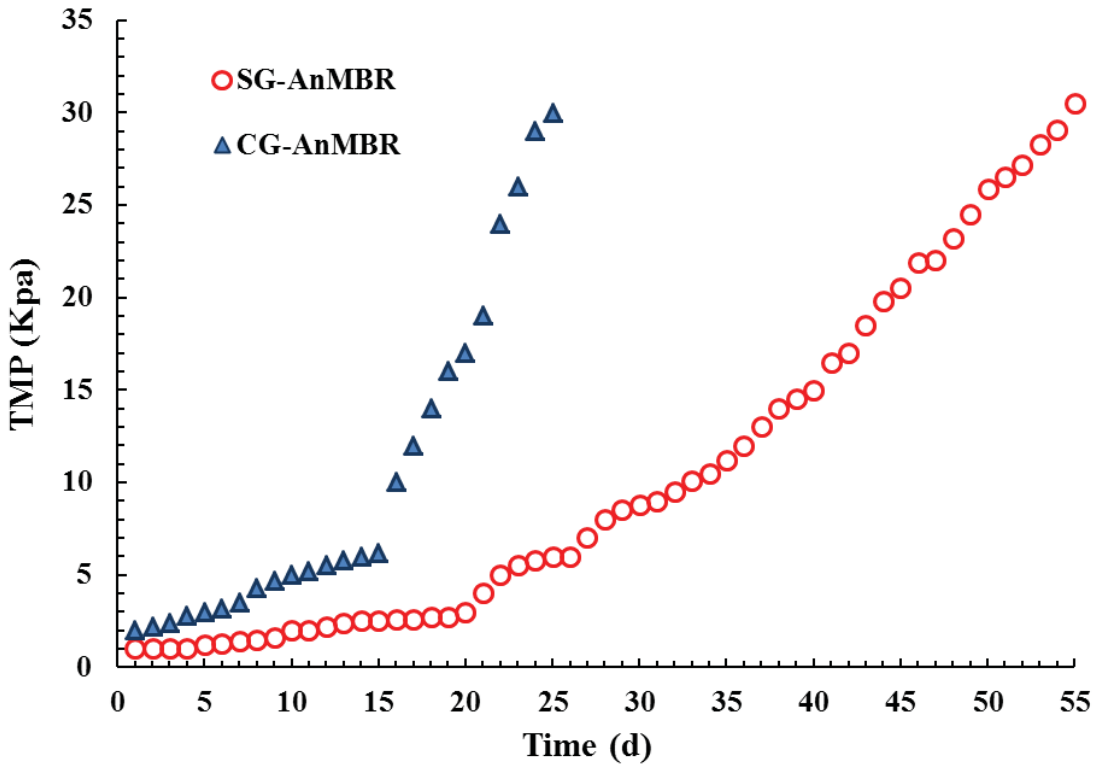

Fig. 2.

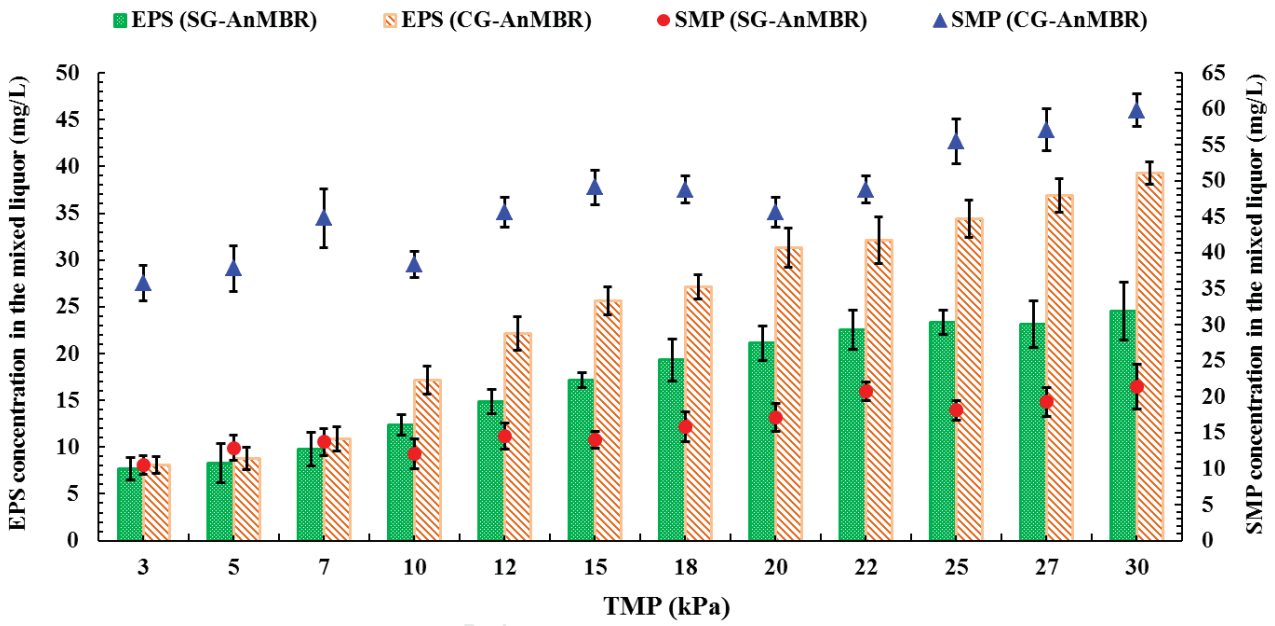

Fig. 3.

Highlights

- Sponge based G-AnMBR is comprehensively studied and evaluated.
- Sponge addition improves granule properties and enhances system performance.
- The SG-AnMBR exhibits less fouling propensity compared to the CG-AnMBR.
- The SG-AnMBR shows no VFA accumulation and yields more biogas.
- The SG-AnMBR presents less organic fractions within the membrane foulants.